

Oscillator Potts machines: An overdamped Langevin model for low-energy sampling of the standard Potts model

Yi Cheng* and Zongli Lin†

Charles L. Brown Department of Electrical and Computer Engineering,
University of Virginia, Charlottesville, Virginia 22904, USA.

(Dated: July 25, 2025)

The standard Potts model is a fundamental model in statistical physics that generalizes the Ising model. Although Ising machines, as Langevin models, have been widely studied for sampling the Ising model, studies of Langevin models for sampling the standard Potts model are still lacking. In this work, we present a compact and physically realizable Langevin model that serves as a sampler for sampling the low-energy spin configurations of the standard Potts model.

Introduction— The Ising model consists of N coupled spins with each spin taking two states ($+1/-1$). In the Ising model, the probability of a given spin configuration occurring is governed by the Boltzmann distribution $p(s) = Z_d^{-1} e^{-\beta H_{\text{Ising}}(s)}$, where β is the inverse temperature, $Z_d = \sum_s e^{-\beta H_{\text{Ising}}(s)}$ is the normalization constant, $s = [s_1 \ s_2 \ \dots \ s_N]^T$, $s_i \in \{+1, -1\}$ represents the i -th spin, $H_{\text{Ising}}(s) = -\sum_{i<j} J_{ij} s_i s_j$ is the Ising Hamiltonian, and J_{ij} denotes the coupling weights between the i -th and the j -th spins. Ising machines are physical platforms that can be used to sample the lower-energy states of the Ising model. In particular, Ising machines typically consist of coupled oscillators, which are designed to admit a potential function $U(x)$ that is a continuous version (or relaxation) of the Ising Hamiltonian, where x is the continuous state of the oscillators. Then, the state of the Ising machine will obey a stationary probability distribution $\Pi(x) = Z^{-1} e^{-\beta U(x)}$ as time goes to infinity, where $Z = \int e^{-\beta U(x)} dx$ is the normalization constant. Numerous studies on Ising machines have shown that, despite continuous-state dynamics, the probability mass concentrates near low-energy spin configurations of the Ising model, efficiently sampling the lower-energy states [1–3]. Due to this property, Ising machines are applicable to solve combinatorial optimization problems, and many studies have demonstrated their effectiveness [4–6]. Since oscillators can be implemented in various physical forms, a wide range of Ising machine architectures have been developed, including coherent Ising machines [7–11], electronic oscillator-based Ising machines [12–16], and others [17–19].

The Potts model is a generalization of the Ising model, and allows the spins to have $q \geq 2$ discrete states. The Potts model is broadly categorized into standard and clock (or planar) types based on the geometric structure of the spin states. The standard Potts model uses arbitrary distinct state values, and the clock Potts model, on the other hand, assigns specific angles on the unit circle as its states. The two models are equivalent when $q = 2$ and $q = 3$, but differ significantly from each other for $q \geq 4$

[20]. For the clock Potts model, dedicated physical platforms have been studied [20, 21]. For the standard Potts model, several studies have attempted to approximate it [22–24], decompose it into multistage [25, 26], or encode it using multiple coupled Ising variables [14, 27, 28]. Therefore, unlike the Ising model, whose physical realizations have been extensively explored through various dedicated Ising machines, there exists no direct and exact physical realization of the standard Potts model.

In this work, we present an overdamped Langevin model that serves as a direct and exact physical realization of the standard Potts model. We refer to the dynamics as oscillator Potts machines (OPMs). Specifically, each oscillator of the OPM is able to take $q \geq 2$ states, and the dynamics admits a potential function that is a continuous version of the standard Potts Hamiltonian $H_{\text{potts}}(s) = -\sum_{i<j} J_{ij} \delta(s_i, s_j)$, where $\delta(s_i, s_j)$ is the Kronecker delta function and $s_i \in \{0, 1, \dots, q-1\}$. In the case of $q = 2$, the OPMs are exactly the oscillator Ising machines (OIMs) that are widely studied [14, 29, 30]. In addition, we note that the existing OIM research focuses on applications to combinatorial optimization problems and has experimentally shown the effectiveness of OIMs. However, theoretical understanding of why and how OIMs achieve such performance remains limited and underdeveloped. Therefore, we provide a theoretical characterization showing that the OPMs/OIMs are indeed biased to sample lower-energy states.

The dynamics— Consider an OPM of N oscillators, with q available discrete states that each oscillator can take. The dynamics of the OPM is given by

$$d[\theta_t]_i = - \left\{ K \sum_{j=1}^N J_{ij} \left(\sum_{m=1}^{q-1} m(q-m) \sin(m([\theta_t]_i - [\theta_t]_j)) \right) + K_s \sin(q[\theta_t]_i) \right\} dt + \sqrt{2\beta^{-1}} dW_t, \quad (1)$$

where $[\theta_t]_i \in \mathbb{T} := [0, 2\pi)$ is the random variable of i -th oscillator, K and K_s are two positive tunable parameters, β is the inverse temperature, and dW_t is the Wiener process. In the absence of the Wiener process, the Langevin model (1) becomes the deterministic dynamics that has q^N equilibrium points. Each component of the equi-

* zss7gw@virginia.edu

† zl5y@virginia.edu

librium point belongs to $\left\{\frac{2k\pi}{q} : k = 0, 1, \dots, q-1\right\}$ (see Supplementary Material). We refer to such equilibrium points as the sampling points. All sampling points exist regardless of the coupling weights J_{ij} and the parameters K and K_s and are asymptotically stable if K_s/K is large enough (see Supplementary Material). In the Supplementary Material, we show that the potential function of (1) is

$$U(\theta) = -\frac{K}{2} \sum_{i < j} J_{ij} \left(2 \sum_{m=1}^{q-1} (q-m) \cos(m(\theta_i - \theta_j)) \right) - \frac{K_s}{q} \sum_{i=1}^N \cos(q\theta_i), \quad (2)$$

which is a continuous version of the standard Potts Hamiltonian with a constant offset. Specifically, there is a component-wise bijection $s[\theta^*]$ between the spin states and the sampling points such that $U(\theta^*)$ is linearly related to $H_{\text{potts}}(s[\theta^*])$.

To better illustrate the dynamics (1), we expand it for $q = 2, 3$, and 4. For $q = 2$, the dynamics is simplified as

$$d[\theta_t]_i = - \left\{ K \sum_{j=1}^N J_{ij} \sin([\theta_t]_i - [\theta_t]_j) + K_s \sin(2[\theta_t]_i) \right\} dt + \sqrt{2\beta^{-1}} dW_t,$$

which becomes the traditional OIM proposed by [14]. In [30], it has been shown that any equilibrium point consisting of $\{0, \pi\}$ is structurally stable with respect to the coupling weights J_{ij} and the parameters K and K_s for the corresponding deterministic dynamics.

For $q = 3$, the dynamics is simplified as

$$d[\theta_t]_i = - \left\{ K \sum_{j=1}^N J_{ij} \left(2 \sin([\theta_t]_i - [\theta_t]_j) + 2 \sin(2[\theta_t]_i - 2[\theta_t]_j) \right) + K_s \sin(3[\theta_t]_i) \right\} dt + \sqrt{2\beta^{-1}} dW_t.$$

It can be verified that any equilibrium point consisting of $\{0, \frac{2\pi}{3}, \frac{4\pi}{3}\}$ is structurally stable with respect to the coupling weights J_{ij} and the parameters K and K_s for the corresponding deterministic dynamics. In addition, we note that when $K_s = 0$, the corresponding deterministic dynamics is similar to oscillatory associative-memory networks that have been studied in [31–33].

For $q = 4$, the dynamics is simplified as

$$d[\theta_t]_i = - \left\{ K \sum_{j=1}^N J_{ij} \left(3 \sin([\theta_t]_i - [\theta_t]_j) + 4 \sin(2[\theta_t]_i - 2[\theta_t]_j) + 3 \sin(3[\theta_t]_i - 3[\theta_t]_j) \right) + K_s \sin(4[\theta_t]_i) \right\} dt + \sqrt{2\beta^{-1}} dW_t.$$

Similarly, any equilibrium point consisting of $\{0, \frac{\pi}{2}, \pi, \frac{3\pi}{2}\}$ is structurally stable with respect to the coupling weights J_{ij} and the parameters K and K_s for the corresponding deterministic dynamics.

Quantization of a Sample— Since the potential function $U(\theta)$ is smooth in \mathbb{T}^N , and $e^{-\beta U(\theta)}$ is Lebesgue integrable in \mathbb{T}^N , the distribution of (1) converges to the distribution with probability density function $\Pi(\theta) = Z^{-1} e^{-\beta U(\theta)}$, where $Z = \int_{\theta \in \mathbb{T}^N} e^{-\beta U(\theta)} d\theta$ [34, 35]. However, obtaining a specified discrete sample, e.g., a sampling point, by (1) is extremely ineffective, since the probability of a sampling point θ^* sampled by (1) is $\mathbb{P}(\theta^*) = \int_{\theta=\theta^*} \Pi(\theta) d\theta = 0$. Therefore, quantization of a sample is a necessary process to make sampling discrete points feasible. We note that quantization is also necessary for many physics-inspired systems to solve combinatorial optimization problems [36–38], since the internal states of physics-inspired systems evolve continuously due to their analog nature, whereas solving combinatorial optimization problems inherently requires discrete solutions. Here, the quantization we consider is that a sample θ_t drawn from (1) falling within a hypercube of the side $2a$ centered at a sampling point θ^* , $(-a, +a)_{\theta^*}^N$, is assigned the value of θ^* . Then, the probability of θ^* occurring after the quantization is

$$\begin{aligned} \mathbb{P}_q(\theta^*) &= \mathbb{P}(\theta_t : \|\theta_t - \theta^*\|_\infty < a) \\ &= Z^{-1} \int_{\theta_t \in (-a, +a)_{\theta^*}^N} e^{-\beta U(\theta_t)} d\theta_t. \end{aligned} \quad (3)$$

In the Supplementary Material, we show that, in the extreme case where $a \rightarrow 0$, $\frac{\mathbb{P}_q(\theta^*)}{\mathbb{P}_q(\phi^*)} = e^{\beta(U(\phi^*) - U(\theta^*))}$ for the sampling points θ^* and ϕ^* . On the one hand, as $a \rightarrow 0$, although the ratio of probabilities between any two sampling points remains exactly the one prescribed by the Boltzmann distribution, the efficiency of discrete sampling becomes extremely low. On the other hand, for larger value of a , while the efficiency of discrete sampling is significantly improved, the resulting distribution (3) no longer preserves the crucial monotonicity property, that is, $U(\theta^*) > U(\phi^*)$ no longer theoretically guarantees $\mathbb{P}_q(\theta^*) < \mathbb{P}_q(\phi^*)$. In the next theorem, we investigate the competition between the monotonicity property of (3) and the efficiency of discrete sampling by evaluating the value of a .

Main Theorem— Consider the potential function (2) and the probability (3) at the sampling points. Let θ^* and ϕ^* be two sampling points. Let $U(\theta^*) > U(\phi^*)$ and $d = U(\theta^*) - U(\phi^*)$. There exists a constant $\mu > 0$ and $\delta = \min \left\{ \sqrt{\frac{2d}{\mu}}, \frac{\pi}{2q} \right\}$ such that for all $a \in (0, \delta)$ and large enough $\frac{K_s}{K}$, $\mathbb{P}_q(\theta^*) < \mathbb{P}_q(\phi^*)$.

The proof of Main Theorem can be found in the Supplementary Material (Proof 7). The efficiency of discrete sampling of (1), denoted by QE, can be characterized by $\text{QE} = \sum_{\theta^* \in \Theta} \mathbb{P}_q(\theta^*)$, where Θ is the set of q^N sampling points. Clearly, $\text{QE} = 0$ without quantization of a sample (the case where $a \rightarrow 0$). The theorem shows that there

exists a fixed $a > 0$ such that the monotonicity property of (3) is preserved. In this case, $a > 0$ guarantees $QE > 0$. In addition, Main Theorem shows that OPMs, with a practical consideration (i.e., quantization of a sample), exhibit the tendency for low-energy sampling of the standard Potts mode (the monotonicity property), which provides a theoretic foundation for OPMs/OIMs to solve combinatorial optimization problems.

Simulation— Consider the standard Potts model of $N = 12$ and $q = 3, 4, 5$, and 6. We numerically demonstrate the effectiveness of the OPM for sampling the low-energy states of the standard Potts model. Since

$$U(\theta^*) = \frac{K(q-1) + q}{2} H_{\text{potts}}(s[\theta^*]) + \text{constant}$$

(see Supplementary Material), we set $K = 2/9, 1/8, 2/25, 1/18$ for $q = 3, 4, 5, 6$, respectively, to ensure that the potential function $U(\theta)$ at the sampling points is equal to the standard Potts Hamiltonian, apart from a constant offset, that is,

$$U(\theta^*) = H_{\text{potts}}(s[\theta^*]) + \text{constant}.$$

In the experiment, we use the Euler–Maruyama method to approximate the OPM, where we set the step size $\epsilon = 0.001$. We fix $\beta = 1$ and $K_s = 20$, and randomly choose the coupling weights J_{ij} . In the quantization process, we set $a = \frac{0.3\pi}{q}$ for $q = 3, 4, 5, 6$. In addition, we add Metropolis–Hastings sampling for a comparison. We keep the number of sampling points obtained by the OPM and that of samples obtained by Metropolis–Hastings sampling the same. The distribution histograms of each state under the two methods are shown in Fig. 1. The figures compare the energy distribution by the two sampling schemes. The histogram labeled “All States” (blue) represents the full enumeration of all configurations. Samples drawn via the OPM (reddish brown)

are biased toward lower-energy states. The Metropolis–Hastings samples (yellow) are even more concentrated in low-energy regions. We note that in OPMs, the parameter K , alongside with the inverse temperature β , governs the degree to which the system favors low-energy states. Thus, we slightly increase K to $K = 1, 3/8, 4/25, 1/12$ for $q = 3, 4, 5, 6$, respectively, with all other parameters remaining the same. The coupling weights are randomly chosen. The corresponding histograms are shown in Fig. 2. We observe that the samples drawn from the OPMs are more concentrated in low-energy regions.

Conclusions— In this work, we present an overdamped Langevin model, the OPM, for sampling the low-energy states of the standard Potts model. The presented OPM can be regarded as an approximation of a discrete sampler for the standard Potts model in a continuous state space in the sense that the potential function of OPM is a continuous version of the standard Potts Hamiltonian. The emergence of OPMs as a new paradigm for the physical implementation of the standard Potts model opens up new avenues for identifying alternative physical platforms that embody its underlying principles. The future extension of OPM can be twofold. From a theoretic perspective, the OPM becomes a class of the Kuramoto model when $K_s = 0$, which could possess rich dynamic behaviors that remain unexplored. From an engineering perspective, the physical implementation of OPMs requires advanced techniques such as higher-order coupling and higher-order harmonic injection locking. As such, the emergence of OPMs has served as a driving force for the development and refinement of these enabling technologies.

Acknowledgments— This material is based upon work supported by the National Science Foundation under grant no. 2328961.

-
- [1] E. Ng, T. Onodera, S. Kako, P. L. McMahon, H. Mabuchi, and Y. Yamamoto, Efficient sampling of ground and low-energy Ising spin configurations with a coherent Ising machine, *Phys. Rev. Res.* **4**, 013009 (2022).
 - [2] F. Böhm, D. Alonso-Urquijo, G. Verschaffelt, and G. Van der Sande, Noise-injected analog Ising machines enable ultrafast statistical sampling and machine learning, *Nat. Commun.* **13**, 5847 (2022).
 - [3] K. Lee, S. Chowdhury, and K. Y. Camsari, Noise-augmented chaotic Ising machines for combinatorial optimization and sampling, *Commun. Phys.* **8**, 35 (2025).
 - [4] N. Mohseni, P. L. McMahon, and T. Byrnes, Ising machines as hardware solvers of combinatorial optimization problems, *Nat. Rev. Phys.* **4**, 363 (2022).
 - [5] C. Bybee, D. Kleyko, D. E. Nikonov, A. Khosrowshahi, B. A. Olshausen, and F. T. Sommer, Efficient optimization with higher-order Ising machines, *Nat. Commun.* **14**, 6033 (2023).
 - [6] J. Sakellariou, A. Askitopoulos, G. Pastras, and S. I. Tsintzos, Encoding arbitrary Ising Hamiltonians on spatial photonic Ising machines, *Phys. Rev. Lett.* **134**, 203801 (2025).
 - [7] T. Inagaki, Y. Haribara, K. Igarashi, T. Sonobe, S. Tamate, T. Honjo, A. Marandi, P. L. McMahon, T. Umeki, K. Enbutsu, *et al.*, A coherent Ising machine for 2000-node optimization problems, *Science* **354**, 603 (2016).
 - [8] P. L. McMahon, A. Marandi, Y. Haribara, R. Hamerly, C. Langrock, S. Tamate, T. Inagaki, H. Takesue, S. Utsunomiya, K. Aihara, *et al.*, A fully programmable 100-spin coherent Ising machine with all-to-all connections, *Science* **354**, 614 (2016).
 - [9] T. Honjo, T. Sonobe, K. Inaba, T. Inagaki, T. Ikuta, Y. Yamada, T. Kazama, K. Enbutsu, T. Umeki, R. Kasahara, *et al.*, 100,000-spin coherent Ising machine, *Sci. Adv.* **7**, eabh0952 (2021).
 - [10] Y. Yamamoto, K. Aihara, T. Leleu, K.-i. Kawarabayashi, S. Kako, M. Fejer, K. Inoue, and H. Takesue, Coherent Ising machines—optical neural networks operating at the

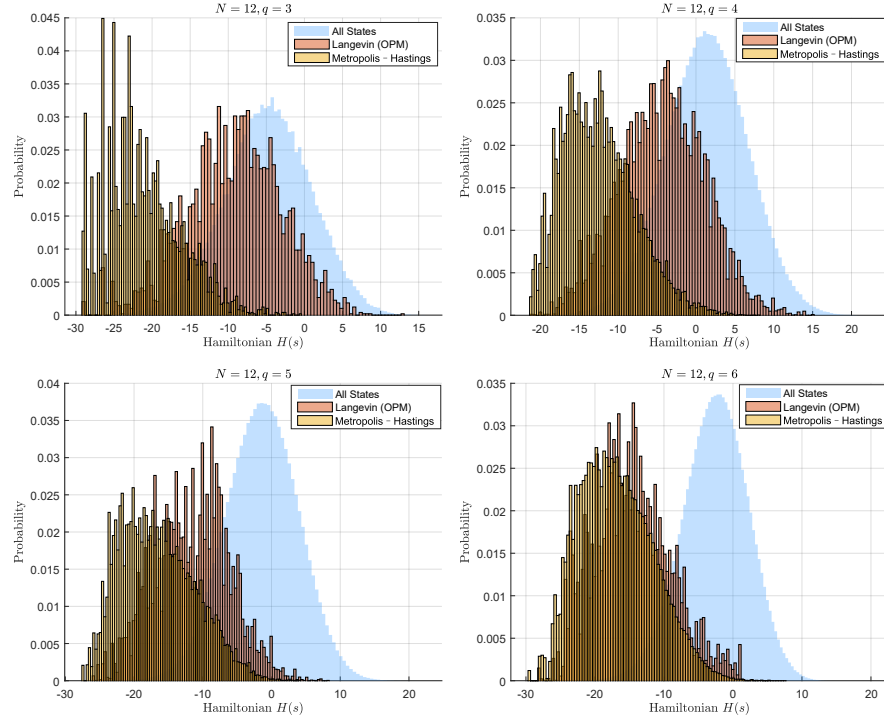


FIG. 1: The distribution of samples: The reddish brown is the distribution of sample obtained from OPM. The yellow is the distribution of sample obtained from Metropolis-Hastings sampling. The light blue is the solution space, which comprises 531, 441, 16, 777, 216, 244, 140, 625, and 2, 176, 782, 336 possible states for $q = 3$, $q = 4$, $q = 5$, and $q = 6$, respectively.

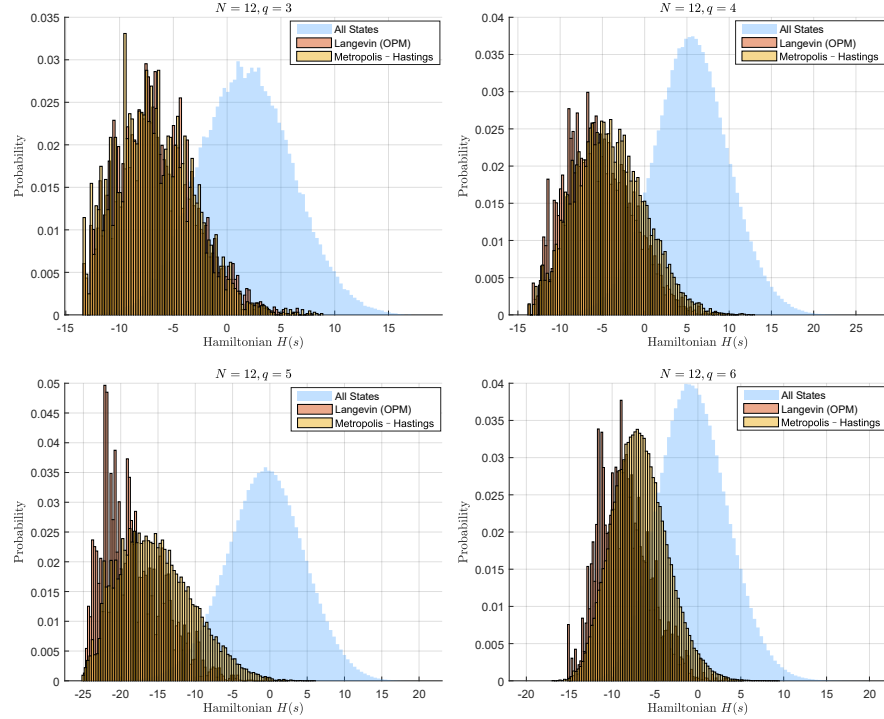


FIG. 2: The distribution of samples: The reddish brown is the distribution of sample obtained from OPM, with slightly larger values of K . The yellow is the distribution of sample obtained from Metropolis-Hastings sampling. The light blue is the solution space.

- N. Zhu, K. Xu, Y. Dai, *et al.*, Large-scale coherent Ising machine based on optoelectronic parametric oscillator, *Light:Sci. Appl.* **11**, 333 (2022).
- [12] O. Maher, M. Jiménez, C. Delacour, N. Harnack, J. Núñez, M. J. Avedillo, B. Linares-Barranco, A. Todri-Sanial, G. Indiveri, and S. Karg, A CMOS-compatible oscillation-based VO2 Ising machine solver, *Nat. Commun.* **15**, 3334 (2024).
- [13] X. Chen, D. Yang, G. Hwang, Y. Dong, B. Cui, D. Wang, H. Chen, N. Lin, W. Zhang, H. Li, *et al.*, Oscillatory neural network-based Ising machine using 2D memristors, *ACS Nano* **18**, 10758 (2024).
- [14] T. Wang, L. Wu, P. Nobel, and J. Roychowdhury, Solving combinatorial optimisation problems using oscillator based Ising machines, *Nat. Comput.* **20**, 287 (2021).
- [15] M. Graber and K. Hofmann, An integrated coupled oscillator network to solve optimization problems, *Commun. Eng.* **3**, 116 (2024).
- [16] Y. Deng, Y. Zhang, X. Zhang, Y. Jiang, X. Chen, Y. Yang, X. Tong, Y. Cai, W. Liu, C. Sun, *et al.*, MEMS oscillators-network-based Ising machine with grouping method, *Adv. Sci.* **11**, 2310096 (2024).
- [17] T. Kanao and H. Goto, High-accuracy Ising machine using Kerr-nonlinear parametric oscillators with local four-body interactions, *npj Quantum Inform.* **7**, 18 (2021).
- [18] J. Ji, X. Ren, J. Gomez, M. K. Bashar, N. Shukla, S. Datta, and P. Zorlutuna, Large-scale cardiac muscle cell-based coupled oscillator network for vertex coloring problem, *Adv. Intell. Syst.* **5**, 2200356 (2023).
- [19] I. Mahboob and H. Yamaguchi, An electromechanical Ising machine, *arXiv preprint arXiv:1505.02467* (2015).
- [20] M. Honari-Latifpour, M. S. Mills, and M.-A. Miri, Combinatorial optimization with photonics-inspired clock models, *Commun. Phys.* **5**, 104 (2022).
- [21] M. Honari-Latifpour and M.-A. Miri, Optical potts machine through networks of three-photon down-conversion oscillators, *Nanophotonics* **9**, 4199 (2020).
- [22] K. Inoue, K. Yoshida, and S. Kitahara, Coherent Potts machine based on an optical loop with a multilevel phase-sensitive amplifier, *Opt. Commun.* **528**, 129022 (2023).
- [23] K. Inaba, T. Inagaki, K. Igarashi, S. Utsunomiya, T. Honjo, T. Ikuta, K. Enbutsu, T. Umeki, R. Kasahara, K. Inoue, *et al.*, Potts model solver based on hybrid physical and digital architecture, *Commun. Phys.* **5**, 137 (2022).
- [24] A. Mallick, M. K. Bashar, Z. Lin, and N. Shukla, Computational models based on synchronized oscillators for solving combinatorial optimization problems, *Phys. Rev. Appl.* **17**, 064064 (2022).
- [25] Y. E. Gonul and B. Taskin, A multi-stage Potts machine based on coupled CMOS ring oscillators, in *2025 Design, Automation & Test in Europe Conference (DATE)* (IEEE, 2025) pp. 1–7.
- [26] A. K. Singh, A. Kapelyan, M. Kim, D. Venturelli, P. L. McMahon, and K. Jamieson, Uplink MIMO detection using Ising machines: A multi-stage Ising approach, *IEEE Trans. Wirel. Commun.* (2024).
- [27] S. Kawakami, Y. Mukasa, S. Bao, D. Ba, J. Arai, S. Yagi, J. Teramoto, and N. Togawa, A constrained graph coloring solver based on Ising machines, in *2023 IEEE International Conference on Consumer Electronics (ICCE)* (IEEE, 2023) pp. 1–6.
- [28] A. Shukla, M. Erementchouk, and P. Mazumder, Non-binary dynamical Ising machines for combinatorial optimization, *Physica D: Nonlinear Phenomena*, 134809 (2025).
- [29] J. Chou, S. Bramhavar, S. Ghosh, and W. Herzog, Analog coupled oscillator based weighted Ising machine, *Sci. Rep.* **9**, 14786 (2019).
- [30] Y. Cheng, M. Khairul Bashar, N. Shukla, and Z. Lin, A control theoretic analysis of oscillator Ising machines, *Chaos* **34** (2024).
- [31] T. Nishikawa, Y.-C. Lai, and F. C. Hoppensteadt, Capacity of oscillatory associative-memory networks with error-free retrieval, *Phys. Rev. Lett.* **92**, 108101 (2004).
- [32] X. Zhao, Z. Li, and X. Xue, Unified approach for applications of oscillatory associative-memory networks with error-free retrieval, *Phys. Rev. E* **108**, 014305 (2023).
- [33] Z. Li, X. Zhao, and X. Zhou, Enhanced error-free retrieval in kuramoto-type associative-memory networks via two-memory configuration, *arXiv preprint arXiv:2505.12223* (2025).
- [34] B. Leimkuhler, C. Matthews, and G. Stoltz, The computation of averages from equilibrium and nonequilibrium Langevin molecular dynamics, *IMA J. Numer. Anal.* **36**, 13 (2016).
- [35] J. Roussel and G. Stoltz, Spectral methods for Langevin dynamics and associated error estimates, *ESAIM:Math. Modell. Numer. Anal.* **52**, 1051 (2018).
- [36] H. Goto, K. Tatsumura, and A. R. Dixon, Combinatorial optimization by simulating adiabatic bifurcations in nonlinear Hamiltonian systems, *Sci. Adv.* **5**, eaav2372 (2019).
- [37] T. Zhang, Q. Tao, B. Liu, and J. Han, A review of simulation algorithms of classical Ising machines for combinatorial optimization, in *2022 IEEE International Symposium on Circuits and Systems (ISCAS)* (IEEE, 2022) pp. 1877–1881.
- [38] J. Wang, D. Ebler, K. M. Wong, D. S. W. Hui, and J. Sun, Bifurcation behaviors shape how continuous physical dynamics solves discrete Ising optimization, *Nat. Commun.* **14**, 2510 (2023).
- [39] F.-Y. Wu, The potts model, *Rev. Mod. Phys.* **54**, 235 (1982).
- [40] M. Chak, T. Lelièvre, G. Stoltz, and U. Vaes, Optimal importance sampling for overdamped Langevin dynamics, *arXiv preprint arXiv:2307.11744* (2023).
- [41] M. Rousset, Y. Xu, and P.-A. Zitt, A weak overdamped limit theorem for Langevin processes, *arXiv preprint arXiv:1709.09866* (2017).

Supplementary Material

Oscillator Potts machines: An overdamped Langevin model for low-energy sampling of the standard Potts model

Yi Cheng* and Zongli Lin†

*Charles L. Brown Department of Electrical and Computer Engineering,
University of Virginia, Charlottesville, Virginia 22904, USA.*

NOMENCLATURE

\mathbb{R}	the set of real numbers
\mathbb{Z}^+	the set of positive integers
\mathbb{T}	the set of phases in a circle: $[0, 2\pi)$
$\mathbb{R}^N, \mathbb{T}^N$	the product sets $\mathbb{R} \times \mathbb{R} \times \cdots \times \mathbb{R}$ and $\mathbb{T} \times \mathbb{T} \times \cdots \times \mathbb{T}$
i	the unit of imaginary
$\Re\{x\}$	the real part of the complex number x
$\Im\{x\}$	the imaginary part of the complex number x
$\text{col}\{x_1, x_2, \dots, x_N\}$	$[x_1^T \ x_2^T \ \dots \ x_N^T]^T$, with column vectors $\{x_1, x_2, \dots, x_N\}$
0_N	the N -dimensional vector $\text{col}\{0, 0, \dots, 0\}$
$\nabla U(\theta)$	the gradient of $U(\theta)$ with respect to θ
$x \in \{a_1, a_2, \dots, a_m\}^N$	$x \in \{\text{col}\{x_1, x_2, \dots, x_N\} : x_i \in \{a_1, a_2, \dots, a_m\}, i = 1, 2, \dots, N\}$
$\ x\ _\infty$	the infinity norm of the vector x
$\ x\ _2$	the 2-norm of the vector x
$[-a, +a]_{\theta^*}^N$	a hypercube of side $2a$ centered at $\theta^* \in \mathbb{T}^N$: $\{\theta \in \mathbb{T}^N : \ \theta - \theta^*\ _\infty \leq a\}$
$(-a, +a)_{\theta^*}^N$	the interior of $[-a, +a]_{\theta^*}^N$: $\{\theta \in \mathbb{T}^N : \ \theta - \theta^*\ _\infty < a\}$

* zss7gw@virginia.edu

† zl5y@virginia.edu

I. INTRODUCTION TO DYNAMICS OF OPMS

We begin by detailing the design of the dynamics of OPMS, with the resulting dynamics serving as the subject of our subsequent analysis.

Consider the standard Potts Hamiltonian of N spins,

$$H_{\text{potts}}(s) = - \sum_{i < j} J_{ij} \delta(s_i, s_j),$$

where $s_i \in \{0, 1, \dots, q-1\}$ is the state of the i -th spin, $q \in \mathbb{Z}^+$ is the number of discrete states available to each spin, $J_{ij} \in \mathbb{R}$ is the coupling weights between the i -th spin and the j -th spin, with $J_{ij} = J_{ji}$ and $J_{ii} = 0$, and

$$\delta(s_i, s_j) = \begin{cases} 1, & \text{if } s_i = s_j, \\ 0, & \text{if } s_i \neq s_j. \end{cases}$$

For the standard Potts model of N spins, the probability of a state $s = \text{col}\{s_1, s_2, \dots, s_N\}$ under a fixed temperature T follows the Boltzmann distribution,

$$p(s) = Z_d^{-1} e^{-\beta H_{\text{potts}}(s)},$$

where $\beta = T^{-1}$, $Z_d = \sum_{s \in S} e^{-\beta H_{\text{potts}}(s)}$, and S is the set of q^N spin configurations. Our goal is to design a Langevin model whose stationary distribution over q^N specified discrete states approximates the Boltzmann distribution or at least is biased to the low-energy spin configurations of the standard Potts Hamiltonian.

For ease in designing the Langevin model, we make a linear transformation for the standard Potts Hamiltonian $H_{\text{potts}}(s)$, that is, $H_{\text{opm}}(s) = (q(q-1) + q)H_{\text{potts}}(s) + \sum_{i < j} J_{ij}q$. It can be verified that $H_{\text{opm}}(s)$ is equal to

$$H_{\text{opm}}(s) = - \sum_{i < j} J_{ij} \tilde{\delta}(s_i, s_j), \tag{1}$$

with

$$\tilde{\delta}(s_i, s_j) = \begin{cases} q(q-1), & \text{if } s_i = s_j, \\ -q, & \text{if } s_i \neq s_j. \end{cases}$$

Instead of considering $H_{\text{potts}}(s)$, we consider its equivalent form $H_{\text{opm}}(s)$ in what follows. Define a potential function $U(\theta)$ as

$$U(\theta) = -\frac{K}{2} \sum_{i < j} J_{ij} \left(2 \sum_{m=1}^{q-1} (q-m) \cos(m(\theta_i - \theta_j)) \right) - \frac{K_s}{q} \sum_{i=1}^N \cos(q\theta_i), \tag{2}$$

where $\theta \in \mathbb{T}^N$, and $K_s, K > 0$ are tunable parameters. The Langevin model is designed to be

$$d\theta_t = -\nabla U(\theta_t)dt + \sqrt{2\beta^{-1}}dW_t, \quad (3)$$

where the random process $\{\theta_t \in \mathbb{T}^N\}_{t \geq 0}$ is the state and dW_t is the Wiener process. Expanding (3), we obtain the dynamics of the OPM

$$d[\theta_t]_i = - \left\{ K \sum_{j=1}^N J_{ij} \left(\sum_{m=1}^{q-1} m(q-m) \sin(m([\theta_t]_i - [\theta_t]_j)) \right) + K_s \sin(q[\theta_t]_i) \right\} dt + \sqrt{2\beta^{-1}}dW_t, \quad (4)$$

where $[\theta_t]_i$ is the i -th component of θ_t .

The OPM (4) possesses several interesting properties. We will discuss them in detail in the following sections. We first summarize these properties as follows.

- The potential function $U(\theta)$ in discrete states $\theta^* \in \left\{ \frac{2k\pi}{q} : k = 0, 1, \dots, q-1 \right\}^N$ coincides with $H_{\text{opm}}(s)$ scaled by a factor of $\frac{K}{2}$ in $s \in \{0, 1, \dots, q-1\}^N$ up to an additive constant, that is, $U(\theta^*) = \frac{K}{2}H_{\text{opm}}(s) + \text{constant}$ (we refer to such discrete states θ^* as sampling points).
- In the absence of the Wiener process, the sampling points are structurally stable equilibrium points (EPs) with respect to the coupling weights J_{ij} and the parameters K and K_s .
- In the absence of the Wiener process, the sampling points are only asymptotically stable EPs as $\frac{K_s}{K} \rightarrow \infty$. In addition, the attractive basin of every sampling point θ^* converges to a hypercube $\left(-\frac{\pi}{q}, +\frac{\pi}{q} \right)_{\theta^*}^N$ as $\frac{K_s}{K} \rightarrow \infty$.
- With the Wiener process, if we perform sampling on (4) and then quantize the sampled values to sampling points, then $U(\theta^*) > U(\phi^*)$ guarantees that the corresponding $\mathbb{P}_q(\theta^*) < \mathbb{P}_q(\phi^*)$, where $\mathbb{P}_q(\theta)$ denotes the probability of θ^* occurring after the quantization. That is, when the OPM is used for discrete sampling, the sampling point with lower energy has a higher probability of occurrence.

The first two properties will be discussed in Section II, the third property will be discussed in Section III, and the last property will be discussed in Section IV.

II. DYNAMIC PROPERTIES OF OPMS

In this section, we focus on dynamic properties of (4) in the absence of the Wiener process,

$$\dot{\theta}_i = -K \sum_{j=1}^N J_{ij} \left(\sum_{m=1}^{q-1} m(q-m) \sin(m(\theta_i - \theta_j)) \right) - K_s \sin(q\theta_i). \quad (5)$$

Specifically, we comment on the connection between the potential function $U(\theta)$ of (5) and the Potts Hamiltonian $H_{\text{opm}}(s)$, and identify structurally stable EPs of (5).

A. The potential function $U(\theta)$ and Potts Hamiltonian $H_{\text{opm}}(s)$

An obvious difference between $U(\theta)$ and $H_{\text{opm}}(s)$ is that $U(\theta)$ is a continuous function while $H_{\text{opm}}(s)$ is a discrete function. However, the next theorem shows that the values of $U(\theta)$ at specified discrete points are linearly related to that of $H_{\text{opm}}(s)$

Theorem 1 *The potential function (2) on sampling points $\theta^* \in \left\{ \frac{2k\pi}{q} : k = 0, 1, \dots, q-1 \right\}^N$ and the Potts Hamiltonian (1) on $s \in \{0, 1, \dots, q-1\}^N$ is related by*

$$U(\theta^*) = \frac{K}{2} H_{\text{opm}}(s[\theta^*]) - \frac{K_s N}{q}, \quad (6)$$

where the mapping $s[\theta^*] : \left\{ \frac{2k\pi}{q} : k = 0, 1, \dots, q-1 \right\}^N \rightarrow \{0, 1, \dots, q-1\}^N$ is a component-wise bijection.

Remark 1 *The mapping $s[\theta^*]$ is a component-wise bijection, that is, a one-to-one correspondence between the distinct components of $\theta^* = \text{col}\{\theta_1^*, \theta_2^*, \dots, \theta_N^*\}$ and those of $s = \text{col}\{s_1, s_2, \dots, s_N\}$. Note that the mapping $s[\theta^*]$ is not unique. Without loss of generality, we consider a mapping $s_i := s_i[\theta^*] = k$ if $\theta_i^* = \frac{2k\pi}{q}$ for $k = 0, 1, \dots, q-1$.*

Proof 1 *The function $f(x) = 2 \sum_{m=1}^{q-1} (q-m) \cos(mx)$ is a periodic function with the smallest positive period $T = 2\pi$. Thus, we only consider $f(x)$ for $x \in \mathbb{T}$. Clearly, as the sum of an arithmetic sequence, $f(x) = q(q-1)$ for $x = 0$. We then focus on $f(x)$ for $x \in \left\{ \frac{2\pi k}{q} : k = 1, 2, \dots, q-1 \right\}$. Let $W_q = \left\{ e^{i \frac{2\pi k}{q}} : k = 1, 2, \dots, q-1 \right\}$. Then, for any $\omega \in W_q$, $\omega^q = 1$ and $\sum_{m=1}^{q-1} \omega^m = -1$. Note that $f(x)$ is the real part of*

$$F(x) = 2 \sum_{m=1}^{q-1} (q-m) e^{imx} = 2q \sum_{m=1}^{q-1} e^{imx} - 2 \sum_{m=1}^{q-1} m e^{imx} := F_1(x) + F_2(x).$$

For $x \in \left\{ \frac{2\pi k}{q} : k = 1, 2, \dots, q-1 \right\}$, let $\omega_x = e^{ix}$. Since $\omega_x \in W_q$,

$$F_1(x) = 2q \sum_{m=1}^{q-1} e^{imx} = 2q \sum_{m=1}^{q-1} \omega_x^m = -2q.$$

Similarly, we have

$$\begin{aligned} F_2(x) &= -2 \sum_{m=1}^{q-1} m e^{imx} \\ &= -2 \sum_{m=1}^{q-1} m \omega_x^m \\ &= \frac{-2\omega_x(1 - q\omega_x^{q-1} + (q-1)\omega_x^q)}{(\omega_x - 1)^2} \\ &= \frac{-2(\omega_x - q\omega_x^q + (q-1)\omega_x^{q+1})}{(\omega_x - 1)^2} \\ &= \frac{-2q(\omega_x - 1)}{(\omega_x - 1)^2} \\ &= \frac{-2q}{\omega_x - 1} \\ &= \frac{-2q}{e^{ix} - 1}, \end{aligned}$$

where, in the third equality, we have used the fact that

$$\begin{aligned} \sum_{m=1}^{q-1} m \omega_x^m &= \omega_x \frac{d(\sum_{m=1}^{q-1} \omega_x^m)}{d\omega_x} \\ &= \frac{\omega_x(1 - q\omega_x^{q-1} + (q-1)\omega_x^q)}{(\omega_x - 1)^2}. \end{aligned}$$

The real part of $F_2(x)$ is given by

$$\begin{aligned} \Re\{F_2(x)\} &= \Re\left\{ \frac{-2q}{\cos(x) - 1 + i \sin(x)} \right\} \\ &= \Re\left\{ \frac{-2q(\cos(x) - 1 - i \sin(x))}{(\cos(x) - 1)^2 + \sin^2(x)} \right\} \\ &= \Re\left\{ q + i \frac{2q \sin(x)}{2 - 2 \cos(x)} \right\} \\ &= q. \end{aligned}$$

Therefore, for $x \in \left\{ \frac{2\pi k}{q} : k = 1, 2, \dots, q-1 \right\}$, $f(x) = \Re\{F(x)\} = \Re\{F_1(x)\} + \Re\{F_2(x)\} = -2q + q = -q$. Then, we obtain

$$f(x) = \begin{cases} q(q-1), & \text{if } x = 0, \\ -q, & \text{if } x \in \left\{ \frac{2\pi k}{q} : k = 1, 2, \dots, q-1 \right\}. \end{cases}$$

Replacing x by $\theta_i^* - \theta_j^*$, we yield

$$f(\theta_i^* - \theta_j^*) = \begin{cases} q(q-1), & \text{if } \theta_i^* - \theta_j^* = 0, \\ -q, & \text{if } \theta_i^* - \theta_j^* \in \left\{ \frac{2\pi k}{q} : k = 1, 2, \dots, q-1 \right\}. \end{cases}$$

Since $\theta_i^*, \theta_j^* \in \left\{ \frac{2\pi k}{q} : k = 0, 1, \dots, q-1 \right\}$, the above equation simplifies to

$$f(\theta_i^* - \theta_j^*) = \begin{cases} q(q-1), & \text{if } \theta_i^* = \theta_j^*, \\ -q, & \text{if } \theta_i^* \neq \theta_j^*. \end{cases}$$

Note that $s_i[\theta^*] = k$ if $\theta_i^* = \frac{2k\pi}{q}$ for $k = 0, 1, \dots, q-1$. Then, $f(\theta_i^* - \theta_j^*) = \tilde{\delta}(s_i[\theta^*], s_j[\theta^*])$.

In addition, $\cos(q\theta_i^*) = 1$, and hence $\sum_{i=1}^N \cos(q\theta_i^*) = N$. Finally, we obtain

$$\begin{aligned} U(\theta^*) &= -\frac{K}{2} \sum_{i < j} J_{ij} \left(2 \sum_{m=1}^{q-1} (q-m) \cos(m(\theta_i - \theta_j)) \right) - \frac{K_s}{q} \sum_{i=1}^N \cos(q\theta_i) \\ &= -\frac{K}{2} \sum_{i < j} J_{ij} f(\theta_i^* - \theta_j^*) - \frac{K_s N}{q} \\ &= -\frac{K}{2} \sum_{i < j} J_{ij} \tilde{\delta}(s_i[\theta^*], s_j[\theta^*]) - \frac{K_s N}{q} \\ &= \frac{K}{2} H_{\text{opm}}(s[\theta^*]) - \frac{K_s N}{q}. \end{aligned}$$

This completes the proof.

Remark 2 Based on Theorem 1 and the linear relation between $H_{\text{opm}}(s)$ and $H_{\text{potts}}(s)$, we have

$$U(\theta^*) = \frac{K(q(q-1) + q)}{2} H_{\text{potts}}(s[\theta^*]) + \frac{K}{2} \sum_{i < j} J_{ij} q - \frac{K_s N}{q}.$$

B. Structurally stable EPs of an OPM

An EP θ^* of an OPM is structurally stable if it remains an EP as the coupling weights J_{ij} and the parameters K and K_s vary. The next theorem identifies the structurally stable EPs of an OPM.

Theorem 2 Consider the dynamics (5).

- For $\frac{q}{2} \in \mathbb{Z}^+$, there are exactly $2q^N$ structurally stable EPs. Half of these EPs are sampling points, and the other half belong to $\left\{ \frac{(2k+1)\pi}{q} : k = 0, 1, \dots, q-1 \right\}^N$.
- For $\frac{q+1}{2} \in \mathbb{Z}^+$, there are $2q^N + q2^N$ structurally stable EPs, where q^N EPs are sampling points, q^N EPs belong to $\left\{ \frac{(2k+1)\pi}{q} : k = 0, 1, \dots, q-1 \right\}^N$, and $q2^N$ EPs belong to $\left\{ \frac{k\pi}{q}, \frac{k\pi}{q} + \pi \right\}^N$ for $k = 0, 1, \dots, q-1$.

Proof 2 Let θ^* be a structurally stable EP. Since θ^* exists for any values of J_{ij} , K and K_s , the following equations hold

$$\sum_{m=1}^{q-1} m(q-m) \sin(m(\theta_i^* - \theta_j^*)) = 0, \quad (7)$$

$$\sin(q\theta_i^*) = 0. \quad (8)$$

First, it can be verified that

$$\theta_i^* \in \left\{ \frac{k\pi}{q} : k = 0, 1, \dots, 2q-1 \right\} \quad (9)$$

is the solution to (8). Note that for any $\theta_i^*, \theta_j^* \in \left\{ \frac{k\pi}{q} : k = 0, 1, \dots, 2q-1 \right\}$, $\theta_i^* - \theta_j^* \in \left\{ \frac{k\pi}{q} : k = 0, 1, \dots, 2q-1 \right\}$. We next show that, for $\frac{q}{2} \in \mathbb{Z}^+$, all the solutions to (7) are given by $\theta_i^* - \theta_j^* \in \left\{ \frac{2k\pi}{q} : k = 0, 1, \dots, q-1 \right\}$, and, for $\frac{q+1}{2} \in \mathbb{Z}^+$, all the solutions to (7) are given by $\theta_i^* - \theta_j^* \in \left\{ \frac{2k\pi}{q} : k = 0, 1, \dots, q-1 \right\} \cup \{\pi\}$.

Consider the function $f(x) = \sum_{m=1}^{q-1} m(q-m) \sin(mx)$. Note that $f(x)$ is the imaginary part of

$$\begin{aligned} F(x) &= \sum_{m=1}^{q-1} m(q-m) e^{imx} \\ &= q \sum_{m=1}^{q-1} m e^{imx} - \sum_{m=1}^{q-1} m^2 e^{imx} \\ &:= F_1(x) + F_2(x). \end{aligned}$$

For $x = 0$, $F(x) = \sum_{m=1}^{q-1} m(q-m) \in \mathbb{R}$, and thus $f(x) = \Im\{F(x)\} = 0$. For $x \in \left\{ \frac{2k\pi}{q} : k = 1, 2, \dots, q-1 \right\}$, let $\omega_x = e^{ix}$. Then

$$F_1(x) = q \sum_{m=1}^{q-1} m e^{imx}$$

$$\begin{aligned}
&= q \sum_{m=1}^{q-1} m \omega_x^m \\
&= \frac{q^2}{\omega_x - 1},
\end{aligned}$$

where we have used the fact that

$$\begin{aligned}
\sum_{m=1}^{q-1} m \omega_x^m &= \omega_x \frac{d(\sum_{m=1}^{q-1} \omega_x^m)}{d\omega_x} \\
&= \frac{\omega_x(1 - q\omega_x^{q-1} + (q-1)\omega_x^q)}{(\omega_x - 1)^2}.
\end{aligned}$$

Similarly, we have

$$\begin{aligned}
F_2(x) &= - \sum_{m=1}^{q-1} m^2 e^{imx} \\
&= - \sum_{m=1}^{q-1} m^2 \omega_x^m \\
&= - \frac{\omega_x(\omega_x + 1) - \omega_x^q(q^2 - (2q^2 - 2q - 1)\omega_x + (q-1)^2\omega_x^2)}{(1 - \omega_x)^3} \\
&= \frac{(2q - q^2)\omega_x + q^2}{(\omega_x - 1)^2},
\end{aligned}$$

where, in the third equality, we have used the fact that

$$\begin{aligned}
\sum_{m=1}^{q-1} m^2 \omega_x^m &= \omega_x \frac{d(\sum_{m=1}^{q-1} m \omega_x^m)}{d\omega_x} \\
&= \frac{\omega_x(\omega_x + 1) - \omega_x^q(q^2 - (2q^2 - 2q - 1)\omega_x + (q-1)^2\omega_x^2)}{(1 - \omega_x)^3}.
\end{aligned}$$

Thus,

$$\begin{aligned}
F(x) &= F_1(x) + F_2(x) \\
&= \frac{q^2}{\omega_x - 1} + \frac{(2q - q^2)\omega_x + q^2}{(\omega_x - 1)^2} \\
&= \frac{2q}{\omega_x + \omega_x^{-1} - 2} \\
&= \frac{q}{\cos(x) - 1}.
\end{aligned}$$

Then, we obtain $f(x) = \Im\{F(x)\} = 0$. Similarly, for $x \in \left\{ \frac{(2k+1)\pi}{q} : k = 0, 1, \dots, q-1 \right\}$, let $\omega_x = e^{ix}$. Note that in this case, $\omega_x^q = -1$. We obtain

$$F_1(x) = \frac{q(2 - q)\omega_x + q^2}{(\omega_x - 1)^2},$$

$$F_2(x) = -\frac{(q^2 + 2 - 2q)\omega_x^2 - (2q^2 - 2q - 2)\omega_x + q^2}{(1 - \omega_x)^3}.$$

Then,

$$\begin{aligned} F(x) &= F_1(x) + F_2(x) \\ &= \frac{-2\omega_x(1 + \omega_x)}{(1 - \omega_x)^3} \\ &= i \frac{\cos\left(\frac{x}{2}\right)}{2\sin^3\left(\frac{x}{2}\right)}, \end{aligned}$$

where we have used the facts that $1 - \omega_x = 1 - e^{ix} = -2ie^{i\frac{x}{2}}\sin(\frac{x}{2})$ and $\omega_x(1 + \omega_x) = 2e^{i\frac{3x}{2}}\cos(\frac{x}{2})$. Thus,

$$f(x) = \Im\{F(x)\} = \frac{\cos\left(\frac{x}{2}\right)}{2\sin^3\left(\frac{x}{2}\right)},$$

which is equal to zero if $x = \pi$. As a result, we conclude that for $x \in \left\{\frac{k\pi}{q} : k = 0, 1, \dots, 2q - 1\right\}$,

$$f(x) = 0 \text{ if } x \in \left\{\frac{2k\pi}{q} : k = 0, 1, \dots, q - 1\right\} \cup \{\pi\}.$$

Note that, for $\frac{q}{2} \in \mathbb{Z}^+$,

$$\left\{\frac{2k\pi}{q} : k = 0, 1, \dots, q - 1\right\} \cup \{\pi\} = \left\{\frac{2k\pi}{q} : k = 0, 1, \dots, q - 1\right\},$$

and hence

$$f(x) = 0, \quad x \in \left\{\frac{2k\pi}{q} : k = 0, 1, \dots, q - 1\right\}.$$

Replace x by $\theta_i^* - \theta_j^*$. We have that, if $\frac{q}{2} \in \mathbb{Z}^+$, then the solution to (7) is given by

$$\theta_i^* - \theta_j^* \in \left\{\frac{2k\pi}{q} : k = 0, 1, \dots, q - 1\right\}, \quad (10)$$

and if $\frac{q+1}{2} \in \mathbb{Z}^+$, then the solution to (7) is given by

$$\theta_i^* - \theta_j^* \in \left\{\frac{2k\pi}{q} : k = 0, 1, \dots, q - 1\right\} \cup \{\pi\}. \quad (11)$$

For $\frac{q}{2} \in \mathbb{Z}^+$, since θ_i^* and θ_j^* satisfy both (9) and (10), it can be verified that either $\theta^* \in \left\{\frac{2k\pi}{q} : k = 0, 1, \dots, q - 1\right\}^N$ or $\theta^* \in \left\{\frac{(2k+1)\pi}{q} : k = 0, 1, \dots, q - 1\right\}^N$. Clearly, there are $2q^N$ such points. For $\frac{q+1}{2} \in \mathbb{Z}^+$, since θ_i^* and θ_j^* satisfy both (9) and (11), it can be verified that either $\theta^* \in \left\{\frac{2k\pi}{q} : k = 0, 1, \dots, q - 1\right\}^N$, $\theta^* \in \left\{\frac{(2k+1)\pi}{q} : k = 0, 1, \dots, q - 1\right\}^N$, or $\theta^* \in \left\{\frac{k\pi}{q}, \frac{k\pi}{q} + \pi\right\}^N$ for $k = 0, 1, \dots, q - 1$. Clearly, there are $2q^N + q2^N$ such points. This completes the proof.

III. STABILITY ANALYSIS OF EPS

In this section, we focus on the stability of EPs of an OPM (5). Theorem 2 shows that many other EPs also exhibit structural stability in addition to sampling points. We note that there are also structurally unstable EPs in (5), although they are difficult to locate. We refer to those structurally stable EPs that are not the sampling points as Type I non-sampling points. On the other hand, we refer to structurally unstable EPs as Type II non-sampling points. In practice, those non-sampling points are unwanted. The next theorem shows that all non-sampling points either are unstable or disappear for large enough $\frac{K_s}{K}$. In contrast, all sampling points are asymptotically stable for large enough $\frac{K_s}{K}$.

Theorem 3 *Consider the dynamics (5). All the sampling points, the Type I non-sampling points, and the Type II non-sampling points are asymptotically stable, unstable, and either unstable or nonexistent, respectively, for large enough $\frac{K_s}{K}$.*

Proof 3 *Given an EP θ^* , the Jacobian matrix of the dynamics (5) at θ^* is given by*

$$A(\theta^*) = KD(\theta^*) - qK_s\Delta(\theta^*), \quad (12)$$

where $D(\theta^*)$ is a symmetric matrix, with diagonal elements

$$D_{ii}(\theta^*) = -\sum_{j=1}^N J_{ij} \left(\sum_{m=1}^{q-1} m^2(q-m) \cos(m(\theta_i^* - \theta_j^*)) \right)$$

and off-diagonal elements

$$D_{ij}(\theta^*) = J_{ij} \sum_{m=1}^{q-1} m^2(q-m) \cos(m(\theta_i^* - \theta_j^*)),$$

and $\Delta(\theta^*)$ is a diagonal matrix with $\Delta_{ii}(\theta^*) = \cos(q\theta_i^*)$. If θ^* is a sampling point, then (12) can be written as $A(\theta^*) = KD(\theta^*) - qK_sI_N$, which is negative definite if and only if

$$\frac{K_s}{K} > \frac{\lambda_N D(\theta^*)}{q}.$$

Choosing $\frac{K_s}{K} > \max_{\theta^* \in \Theta_1} \left\{ \frac{\lambda_N D(\theta^*)}{q} \right\}$, where Θ_1 is the set of q^N sampling points, makes all sampling points asymptotically stable. If θ^* is a Type I non-sampling point, the corresponding Jacobian matrix is $A(\theta^*) = KD(\theta^*) - qK_s\Delta(\theta^*)$, with at least one diagonal entry of $\Delta(\theta^*)$, say $\Delta_{11}(\theta^*)$, equal to -1 . Thus, $A_{11}(\theta^*) = KD_{11}(\theta^*) + qK_s$, which is positive if $\frac{K_s}{K} > \frac{-D_{11}(\theta^*)}{q}$.

Choosing $\frac{K_s}{K} > \max_{\theta^* \in \Theta_2} \left\{ \frac{-D_{11}(\theta^*)}{q} \right\}$, where Θ_2 is the set of all Type I non-sampling points, makes all Type I non-sampling points unstable. If θ^* is a Type II non-sampling point, we consider two cases. In the first case, $\theta^* \in \left\{ \frac{k\pi}{q} : k = 0, 1, \dots, 2q-1 \right\}^N$, and there are at least two components of θ^* in $\left\{ \frac{2k\pi}{q} : 0, 1, \dots, q-1 \right\}$ and $\left\{ \frac{(2k+1)\pi}{q} : k = 0, 1, \dots, q-1 \right\}$ each. Since there is at least one phase, say θ_1^* , in $\left\{ \frac{(2k+1)\pi}{q} : k = 0, 1, \dots, q-1 \right\}$, the instability of the point for large enough $\frac{K_s}{K}$ follows the same argument of that of Type I non-sampling points. In the second case, $\theta_i^* \notin \left\{ \frac{k\pi}{q} : k = 0, 1, \dots, 2q-1 \right\}$ for at least one $i, i = 1, 2, \dots, N$. For such phases, they satisfy

$$-K \sum_{j=1}^N J_{ij} \left(\sum_{m=1}^{q-1} m(q-m) \sin(m(\theta_i^* - \theta_j^*)) \right) = K_s \sin(q\theta_i^*) \neq 0,$$

that is,

$$\begin{aligned} \sin(q\theta_i^*) &= -\frac{K}{K_s} \sum_{j=1}^N J_{ij} \left(\sum_{m=1}^{q-1} m(q-m) \sin(m(\theta_i^* - \theta_j^*)) \right) \\ &:= -\frac{K}{K_s} \sum_{j=1}^N J_{ij} f(\theta_i^* - \theta_j^*) \neq 0. \end{aligned}$$

Note that $f(\theta_i - \theta_j)$ is uniformly bounded with respect to $\theta_i - \theta_j$. Let $\rho_{ij} := \sup_{\theta_i, \theta_j} |J_{ij} f(\theta_i - \theta_j)|$, and $\rho_i = \sum_{j=1}^N \rho_{ij} < \infty$. Note that, by the triangle inequality and the subadditivity of the superior, $\sup_{\theta_i, \theta_j} |\sum_{j=1}^N J_{ij} f(\theta_i - \theta_j)| \leq \rho_i$. Then, for any $\epsilon > 0$, choosing $\frac{K_s}{K} > \frac{\rho_i}{\epsilon}$ results in

$$|\sin(q\theta_i^*)| = \left| \frac{K}{K_s} \sum_{j=1}^N J_{ij} f(\theta_i^* - \theta_j^*) \right| < \epsilon,$$

which implies that there exists $k_i \in \mathbb{Z}^+$ such that for any $\epsilon \in (0, 1)$,

$$|q\theta_i^* - k_i\pi| < \arcsin(\epsilon). \quad (13)$$

If $\frac{k_i+1}{2} \in \mathbb{Z}^+$ for at least one i , say $i = 1$, then $-1 < \cos(q\theta_1^*) < \cos(k_1\pi + \arcsin(\epsilon)) = -\sqrt{1-\epsilon^2}$. Thus, $A_{11}(\theta^*) = KD_{11}(\theta^*) - qK_s \cos(\theta_1^*) > KD_{11}(\theta^*) + qK_s \sqrt{1-\epsilon^2}$, which is positive if $\frac{K_s}{K} > -\frac{D_{11}(\theta_1^*)}{q\sqrt{1-\epsilon^2}}$. As a result, choosing $\frac{K_s}{K} > \max \left\{ \frac{\rho_1}{\epsilon}, -\frac{D_{11}(\theta_1^*)}{q\sqrt{1-\epsilon^2}} \right\}$ makes θ^* unstable. If $\frac{k_i}{2} \in \mathbb{Z}^+$ for all i , let $\phi^* = \text{col} \left\{ \frac{k_1\pi}{q}, \frac{k_2\pi}{q}, \dots, \frac{k_N\pi}{q} \right\}$. Note that ϕ^* is a sampling point. Then, (13) holds for all i by choosing $\frac{K_s}{K} > \max_i \left\{ \frac{\rho_i}{\epsilon} \right\}$, resulting in $\|\theta^* - \phi^*\|_\infty = \max_i \{|\theta_i^* - \phi_i^*|\} < \frac{\arcsin(\epsilon)}{q}$. Since ϕ^* is asymptotically stable for $\frac{K_s}{K} > \frac{\lambda_N(D(\phi^*))}{q}$, there exists $\epsilon_1 \in \left(0, \frac{\pi}{2q}\right)$ such that $\mathcal{D} = \{\theta \in \mathbb{T}^N : \|\theta - \phi^*\|_\infty < \epsilon_1\}$ is an estimated attractive basin of ϕ^* . As a result,

choosing $\frac{K_s}{K} > \max \left\{ \max_i \left\{ \frac{\rho_i}{\epsilon} \right\}, \frac{\lambda_N(D(\phi^*))}{q} \right\}$, with $\epsilon < \sin(q\epsilon_1)$, makes θ^* nonexistent, since such value of $\frac{K_s}{K}$ will cause $\|\theta^* - \phi^*\|_\infty < \epsilon_1$, implying that θ^* is located in the attractive basin of ϕ^* , which contradicts the definition of the attractive basin. This completes the proof.

The attractive basin is an important dynamic property of asymptotically stable EPs. The next theorem characterizes the limit of the attractive basin for a sampling point as $\frac{K_s}{K} \rightarrow \infty$.

Theorem 4 *Consider the dynamics (5). The attractive basin of each sampling point θ^* converges to a hypercube $\left(-\frac{\pi}{q}, +\frac{\pi}{q}\right)_{\theta^*}^N$ as $\frac{K_s}{K} \rightarrow \infty$.*

Proof 4 *By Theorem 3, all sampling points are asymptotically stable for large enough $\frac{K_s}{K}$. Thus, the attractive basin of each sampling point exists for $\frac{K_s}{K} \rightarrow \infty$. Consider the following dynamics*

$$\dot{\theta}_i = -K_s \sin(q\theta_i), \quad (14)$$

where $\theta_i \in \mathbb{T}$. It can be verified that $(2q)^N$ points belonging to $\left\{ \frac{k\pi}{q} : k = 0, 1, \dots, 2q-1 \right\}^N$ constitute all EPs of (14). In addition, a simple calculation shows that EPs belonging to $\left\{ \frac{2k\pi}{q} : k = 0, 1, \dots, q-1 \right\}^N$ are asymptotically stable and others are unstable for any $K_s > 0$. Thus, for each asymptotically stable EP θ^* of (14), the attractive basin is a hypercube $\left(-\frac{\pi}{q}, +\frac{\pi}{q}\right)_{\theta^*}^N$. The potential function of (14) can be verified as

$$W(\theta; K_s) = -\frac{K_s}{q} \left(\sum_{i=1}^N \cos(q\theta_i) + h \right),$$

where h is a constant. Recall that

$$\begin{aligned} U(\theta; K_s, K) &= -K \sum_{i < j} J_{ij} \left(2 \sum_{m=1}^{q-1} (q-m) \cos(m(\theta_i - \theta_j)) \right) - \frac{K_s}{q} \left(\sum_{i=1}^N \cos(q\theta_i) + h \right) \\ &:= G(\theta; K) + W(\theta; K_s) \end{aligned}$$

is the potential function of (5). In what follows, we analyze the potential function $U(\theta)$ for $\frac{K_s}{K} \rightarrow \infty$. Without loss of generality, we fix $K = 1$ and let $K_s \rightarrow \infty$. Specifically, we will show that $\lim_{K_s \rightarrow \infty} \frac{U(\theta; K_s, 1)}{W(\theta; K_s)} = 1$ uniformly with respect to θ . Since $\sum_{i=1}^N \cos(q\theta_i) \geq -N$, we can choose $h > N$ such that $W(\theta; K_s) > 0$ for all θ and K_s , thus $p := \inf_{\theta} \left(\sum_{i=1}^N \cos(q\theta_i) + h \right) > 0$. Since $G(\theta; 1)$ is uniformly bounded with respect to θ , $\kappa := \sup_{\theta} |G(\theta; 1)| < \infty$. For every $\epsilon > 0$ and $\theta \in \mathbb{T}^N$, choosing $K_s > \frac{q\kappa}{p\epsilon}$ results in

$$\sup_{\theta} \left| \frac{U(\theta; K_s, 1)}{W(\theta; K_s)} - 1 \right| = \sup_{\theta} \left| \frac{G(\theta; 1) + W(\theta; K_s)}{W(\theta; K_s)} - 1 \right|$$

$$\begin{aligned}
&= \sup_{\theta} \left| \frac{G(\theta; 1)}{W(\theta; K_s)} \right| \\
&\leq \sup_{\theta} \left| \frac{\kappa}{W(\theta; K_s)} \right| \\
&= \sup_{\theta} \left| \frac{\kappa}{\frac{K_s}{q} \left(\sum_{i=1}^N \cos(q\theta_i) + h \right)} \right| \\
&< \sup_{\theta} \left| \frac{p\epsilon}{\left(\sum_{i=1}^N \cos(q\theta_i) + h \right)} \right| \\
&\leq \epsilon
\end{aligned}$$

Thus, $\lim_{K_s \rightarrow \infty} \frac{U(\theta; K_s, 1)}{W(\theta; K_s)} = 1$ uniformly with respect to θ . This means that the potential landscapes of (5) and (14) converge to the same landscape as K_s increases. Note that the asymptotically stable EPs of (14) and the sampling points of (5) are the same. Finally, we conclude that the sampling point θ^* of (5) has the attractive basin converging to a hypercube $\left(-\frac{\pi}{q}, +\frac{\pi}{q}\right)_{\theta^*}^N$ as $\frac{K_s}{K} \rightarrow \infty$. This completes the proof.

Example. We use numerical simulation to validate Theorem 4. Consider an OPM of three oscillators with $q = 3$. Fig. 1 shows the phase portrait around $\theta^* = \text{col}\{0, 0, 0\}$ and $\phi^* = \text{col}\{0, \frac{2\pi}{3}, 0\}$ when $K = 1, K_s = 50$. Fig. 2 shows the evolution of the phase portrait on the (θ_1, θ_2) plane as K_s ranges from one to 50.

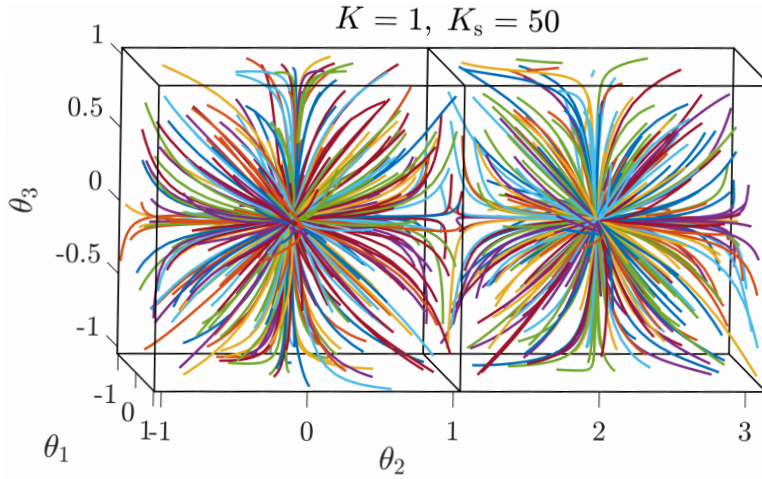


FIG. 1: Phase portrait

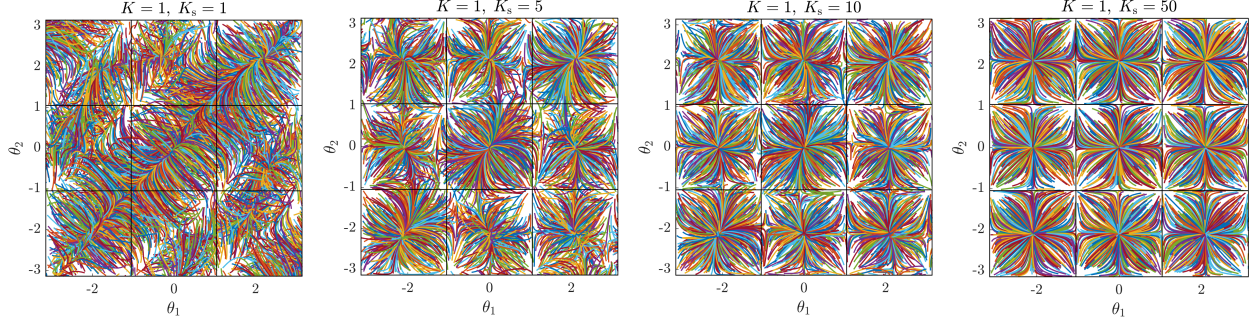


FIG. 2: Phase portraits of one dimension when $q = 3$. The attractive basins of EPs converge to a hypercube as K_s increases

IV. QUANTIZATION OF A SAMPLE

By performing the dynamics (4), the distribution of θ_t coverages to a stationary distribution with the probability density function

$$\Pi(\theta) = Z^{-1} e^{-\beta U(\theta)},$$

where $Z = \int_{\theta \in \mathbb{T}^N} e^{-\beta U(\theta)} d\theta$. Clearly, $\Pi(\theta)$ is continuous in θ , which is different from the probability mass function $p(s)$ considered in the standard Potts model. For the Langevin model (4), sampling θ^* is extremely ineffective, since the probability of the sampling point θ^* is $\mathbb{P}(\theta^*) = \int_{\theta=\theta^*} \Pi(\theta) d\theta = 0$. Therefore, we may take quantization on a sample θ_t to increase the probability of sampling points, which is also commonly used in Ising machines for combinatorial optimization problems. Here, the quantization we considered is that a sample θ_t falling within a hypercube $(-a, +a)_{\theta^*}^N$ is assigned to the value of θ^* , where $a \in (0, \frac{\pi}{q})$ is a constant, and θ^* is a sampling point. After the quantization, the probability of the sampling point θ^* occurring is

$$\begin{aligned} \mathbb{P}_q(\theta^*) &= \mathbb{P}(\theta_t : \|\theta_t - \theta^*\|_\infty < a) \\ &= Z^{-1} \int_{\theta_t \in (-a, +a)_{\theta^*}^N} e^{-\beta U(\theta_t)} d\theta_t. \end{aligned} \quad (15)$$

When $a \rightarrow 0$, it can be shown that $\frac{\mathbb{P}_q(\theta^*)}{\mathbb{P}_q(\phi^*)} = e^{\beta(U(\phi^*) - U(\theta^*))}$ (see Proposition 1 below), which is the Boltzmann ratio for the potential functions. As we discussed earlier, a smaller value of a leads to a more ineffective discrete sampling. In contrast, a large value of a improves the efficiency of discrete sampling, but cannot theoretically guarantee that the distribution (15) has the monotonicity property, that is, $U(\theta^*) > U(\phi^*)$ cannot theoretically guarantee that

$\mathbb{P}_q(\theta^*) < \mathbb{P}_q(\phi^*)$ for a large value of $a \in \left(0, \frac{\pi}{q}\right)$. In this section, we investigate whether a favorable trade-off exists between effective discrete sampling and the monotonicity property of the distribution (15). Our main result is shown in Theorem 5. Before we state the main result, we introduce a proposition for showing the property of (15) in an extreme case and a lemma for preliminary of the main result.

Remark 3 Let Θ be the set of q^N sampling points. $\sum_{\theta^* \in \Theta} \mathbb{P}_q(\theta^*) < 1$ since the region $\bigcup_{\theta^* \in \Theta} (-a, +a)_{\theta^*}^N$ is a subset of \mathbb{T}^N for any $a \in \left(0, \frac{\pi}{q}\right)$. Therefore, in the finite set Θ , we can define a renormalized discrete distribution over Θ as

$$\tilde{\mathbb{P}}(\theta^*) = \frac{\mathbb{P}_q(\theta^*)}{\sum_{\theta \in \Theta} \mathbb{P}_q(\theta)}.$$

This ensures that $\sum_{\theta \in \Theta} \tilde{P}(\theta) = 1$.

Proposition 1 Consider two sampling points θ^* and ϕ^* of the OPM and the probability (15). Then,

$$\lim_{a \rightarrow 0} \frac{\mathbb{P}_q(\theta^*)}{\mathbb{P}_q(\phi^*)} = e^{\beta(U(\phi^*) - U(\theta^*))}.$$

Proof 5 Let $y = \theta - \theta^*$. Then, we have $\Pi(y + \theta^*) = \Pi(\theta)$. Since $\Pi(\theta)$ is differentiable, by the Taylor expansion with Lagrange remainder around θ^* ,

$$\Pi(y + \theta^*) = \Pi(\theta^*) + \nabla \Pi^T(\theta^*)y + R_2(y),$$

where $|R_2(y)| \leq C\|y\|_2^2$ for small $\|y\|_2$ and a constant C . Then, for small enough $\|y\|_2$,

$$\begin{aligned} \int_{y \in (-a, +a)_{0_N}^N} \Pi(y + \theta^*) dy &= \int_{y \in (-a, +a)_{0_N}^N} \Pi(\theta^*) dy + \int_{y \in (-a, +a)_{0_N}^N} \nabla \Pi^T(\theta^*)y dy \\ &\quad + \int_{y \in (-a, +a)_{0_N}^N} R_2(y) dy \\ &= \int_{y \in (-a, +a)_{0_N}^N} \Pi(\theta^*) dy + \int_{y \in (-a, +a)_{0_N}^N} R_2(y) dy \\ &= (2a)^N \Pi(\theta^*) + O(a^{N+2}), \end{aligned}$$

where we have used the facts that $\nabla \Pi^T(\theta^*)y$ is an odd function with respect to y and $(-a, +a)_{0_N}^N$ is a symmetric region with respect to y . In addition, we have also used the fact that, for small enough $\|y\|_2$,

$$\left| \int_{y \in (-a, +a)_{0_N}^N} R_2(y) dy \right| \leq \left| \int_{y \in (-a, +a)_{0_N}^N} C\|y\|_2^2 dy \right|$$

$$\begin{aligned}
&\leq \left| \int_{y \in (-a, +a)_{0_N}^N} CN \|y\|_\infty^2 dy \right| \\
&\leq \left| \int_{y \in (-a, +a)_{0_N}^N} CN a^2 dy \right| \\
&= 2^N CN a^{N+2}.
\end{aligned}$$

Therefore,

$$\begin{aligned}
\lim_{a \rightarrow 0} \frac{\mathbb{P}_q(\theta^*)}{\mathbb{P}_q(\phi^*)} &= \lim_{a \rightarrow 0} \frac{\int_{y \in (-a, +a)_{0_N}^N} \Pi(y + \theta^*) dy}{\int_{y \in (-a, +a)_{0_N}^N} \Pi(y + \phi^*) dy} \\
&= \lim_{a \rightarrow 0} \frac{(2a)^N \Pi(\theta^*) + O(a^{N+2})}{(2a)^N \Pi(\phi^*) + O(a^{N+2})} \\
&= \lim_{a \rightarrow 0} \frac{\Pi(\theta^*) + \frac{O(a^{N+2})}{(2a)^N}}{\Pi(\phi^*) + \frac{O(a^{N+2})}{(2a)^N}} \\
&= \frac{\Pi(\theta^*)}{\Pi(\phi^*)} \\
&= e^{\beta(U(\phi^*) - U(\theta^*))}.
\end{aligned}$$

This completes the proof.

Lemma 1 Consider a sampling point θ^* and a hypercube $(-a, +a)_{\theta^*}^N$. For any $a \in (0, \frac{\pi}{2q})$, the potential function (2) is strongly convex in $(-a, +a)_{\theta^*}^N$ for large enough $\frac{K_s}{K}$. In addition, θ^* is the unique minimum of $U(\theta)$ in $(-a, +a)_{\theta^*}^N$.

Proof 6 The Hessian matrix of $U(\theta)$ is given by

$$\nabla^2 U(\theta) = -A(\theta) = -KD(\theta) + qK_s \Delta(\theta),$$

where $D(\theta)$ is a symmetric matrix given in Proof of Theorem 3, and $\Delta(\theta)$ is a diagonal matrix whose diagonal is $\Delta_{ii}(\theta) = \cos(q\theta_i)$. Since $\theta_i^* \in \left\{ \frac{2k\pi}{q} : k = 0, 1, \dots, q-1 \right\}$ and $a \in (0, \frac{\pi}{2q})$, it can be verified that $\cos(q\theta_i) > 0$ for any $\theta_i \in [\theta_i^* - a, \theta_i^* + a]$. Given a point $\theta \in [-a, +a]_{\theta^*}^N$, let $\kappa = \max_i \{|D_{ii}(\theta)|\}$, $\varsigma = \max_i \{|\sum_{j \neq i, j=1}^N D_{ij}(\theta)|\}$, and $g = \min_i \{\Delta_{ii}(\theta)\}$. Note that $g > 0$. Choosing $\frac{K_s}{K} > \frac{\kappa + \varsigma}{qg}$ ensures that $\nabla^2 U(\theta)$ is a diagonal dominance matrix for any $\theta \in [-a, +a]_{\theta^*}^N$, where $a \in (0, \frac{\pi}{2q})$. Note that $\nabla^2 U(\theta)$ is symmetric. By Gershgorin Disc Theorem, we see that $\nabla^2 U(\theta)$ is positive definite, and therefore $U(\theta)$ is strictly convex in $[-a, +a]_{\theta^*}^N$ as $[-a, +a]_{\theta^*}^N$ is the convex set. Given that the hypercube $[-a, +a]_{\theta^*}^N$ is a compact set, $U(\theta)$ is strongly convex in $[-a, +a]_{\theta^*}^N$. Since $(-a, +a)_{\theta^*}^N \subset [-a, +a]_{\theta^*}^N$, $U(\theta)$ is strongly

convex in $(-a, +a)_{\theta^*}^N$. By Theorem 2, $\nabla U(\theta^*) = 0_N$, and therefore θ^* is the unique minimum of $U(\theta)$ in $(-a, +a)_{\theta^*}^N$. This completes the proof.

Theorem 5 Consider the potential function (2) and the distribution (15) at the sampling points. Let θ^* and ϕ^* be two sampling points. Let $U(\theta^*) > U(\phi^*)$ and $d = U(\theta^*) - U(\phi^*)$. There exists a constant $\mu > 0$ and $\delta = \min \left\{ \sqrt{\frac{2d}{\mu}}, \frac{\pi}{2q} \right\}$ such that for all $a \in (0, \delta)$ and large enough $\frac{K_s}{K}$, $\mathbb{P}_q(\theta^*) < \mathbb{P}_q(\phi^*)$.

Proof 7 Let $\gamma^* = \theta^* - \phi^*$. Then $U(\theta)$ in $(-a, +a)_{\phi^*}^N$ is pointwise equal to $U(\theta - \gamma^*)$ in $(-a, +a)_{\theta^*}^N$. Let $W(\theta) = U(\theta - \gamma^*)$. By Lemma 1, we can choose $\frac{K_s}{K}$ large enough such that both $U(\theta)$ and $W(\theta)$ are strongly convex in $(-a, +a)_{\theta^*}^N$ for any $a \in \left(0, \frac{\pi}{2q}\right)$, where θ^* is the common unique minimum. Let $F(\theta) = U(\theta) - W(\theta)$ and $d = F(\theta^*)$. Note that $W(\theta^*) = U(\phi^*) < U(\theta^*)$, and hence $d > 0$. Since $U(\theta)$ is strongly convex for $\theta \in (-a, +a)_{\theta^*}^N$ with $a \in \left(0, \frac{\pi}{2q}\right)$, there exists $m_1 > 0$ such that for any $\theta \in (-a, +a)_{\theta^*}^N$ with $a \in \left(0, \frac{\pi}{2q}\right)$,

$$\begin{aligned} U(\theta) &\geq U(\theta^*) + \nabla U(\theta^*)^T(\theta - \theta^*) + \frac{m_1}{2} \|\theta - \theta^*\|_2^2 \\ &\geq U(\theta^*) + \frac{m_1}{2} \|\theta - \theta^*\|_\infty^2. \end{aligned} \quad (16)$$

By the Taylor expansion with the Lagrange form of reminder, $W(\theta)$ can be expressed as

$$\begin{aligned} W(\theta) &= W(\theta^*) + \nabla W(\theta^*)^T(\theta - \theta^*) + \frac{1}{2}(\theta - \theta^*)^T \nabla^2 W(\xi)(\theta - \theta^*) \\ &= W(\theta^*) + \frac{1}{2}(\theta - \theta^*)^T \nabla^2 W(\xi)(\theta - \theta^*), \end{aligned} \quad (17)$$

for some ξ lies on the interval between θ and θ^* . Let $m_2 = \max_{\theta \in [-a, +a]_{\theta^*}^N} \lambda_N(\nabla^2 W(\theta))$. In view of (16) and (17), we have

$$\begin{aligned} F(\theta) &= U(\theta) - W(\theta) \\ &\geq U(\theta^*) - W(\theta^*) + \frac{m_1}{2} \|\theta - \theta^*\|_\infty^2 - \frac{m_2}{2} \|\theta - \theta^*\|_2^2 \\ &= d + \frac{m_1}{2} \|\theta - \theta^*\|_\infty^2 - \frac{m_2}{2} \|\theta - \theta^*\|_2^2 \\ &\geq d + \frac{m_1 - m_2 N}{2} \|\theta - \theta^*\|_\infty^2, \end{aligned}$$

where we have used the fact that $\|\theta - \theta^*\|_2^2 \leq N \|\theta - \theta^*\|_\infty^2$. If $m_1 \geq m_2 N$, we have $F(\theta) > 0$ for all $\theta \in (-a, +a)_{\theta^*}^N$ with $a \in \left(0, \frac{\pi}{2q}\right)$. If $m_1 < m_2 N$, $F(\theta) > 0$ for

$$\theta \in \left\{ \theta : \|\theta - \theta^*\|_\infty < \sqrt{\frac{2d}{m_2 N - m_1}} := \sqrt{\frac{2d}{\mu}} \right\}.$$

In other words, there exist $\mu > 0$ and $\delta = \min \left\{ \sqrt{\frac{2d}{\mu}}, \frac{\pi}{2q} \right\}$ such that for any $a \in (0, \delta)$ and any $\theta \in (-a, +a)_{\theta^*}^N$, $F(\theta) > 0$, that is, $U(\theta) > W(\theta) = U(\theta - \gamma^*)$. Thus, $e^{-\beta U(\theta)} < e^{-\beta U(\theta - \gamma^*)}$ for any $\theta \in (-a, +a)_{\theta^*}^N$. Then, by the monotonicity of the integral,

$$\begin{aligned}
\frac{\mathbb{P}_q(\theta^*)}{\mathbb{P}_q(\phi^*)} &= \frac{\mathbb{P}_q(\theta^*)}{\mathbb{P}_q(\theta^* - \gamma^*)} \\
&= \frac{\int_{\theta \in (-a, +a)_{\theta^*}^N} Z^{-1} e^{-\beta U(\theta)} d\theta}{\int_{\theta \in (-a, +a)_{\theta^* - \gamma^*}^N} Z^{-1} e^{-\beta U(\theta)} d\theta} \\
&= \frac{\int_{\theta \in (-a, +a)_{\theta^*}^N} e^{-\beta U(\theta)} d\theta}{\int_{\theta \in (-a, +a)_{\theta^* - \gamma^*}^N} e^{-\beta U(\theta)} d\theta} \\
&= \frac{\int_{\theta \in (-a, +a)_{\theta^*}^N} e^{-\beta U(\theta)} d\theta}{\int_{\theta \in (-a, +a)_{\theta^*}^N} e^{-\beta U(\theta - \gamma^*)} d\theta} \\
&< 1.
\end{aligned}$$

This completes the proof.

To demonstrate Theorem 5, consider an OPM of two oscillators with $q = 3$. The coupling weight $J_{12} = -1$. Fix $K = 1$ and $K_s = 15$. Consider $\theta^* = \{0, 0\}$ and $\phi^* = \{\frac{2\pi}{3}, 0\}$. A simple calculation shows that $U(\theta^*) = -8$ and $U(\phi^*) = -11$. Let $\gamma^* = \theta^* - \phi^*$ and $W(\theta) = U(\theta - \gamma^*)$. We have $W(\theta)$ in the region of $(-\frac{\pi}{3}, +\frac{\pi}{3})_{\theta^*}^2$ pointwise equal to $U(\theta)$ in the region of $(-\frac{\pi}{3}, +\frac{\pi}{3})_{\phi^*}^2$. Clearly, $W(\theta^*) = U(\phi^*) = -11$. Fig. 3 shows the manifolds of $U(\theta)$ and $W(\theta)$ in the region of $(-\frac{\pi}{3}, +\frac{\pi}{3})_{\theta^*}^2$. We observe that $U(\theta) > W(\theta)$ in the black rectangle, where the black rectangle is $(-\frac{\pi}{6}, +\frac{\pi}{6})_{\theta^*}^2$.

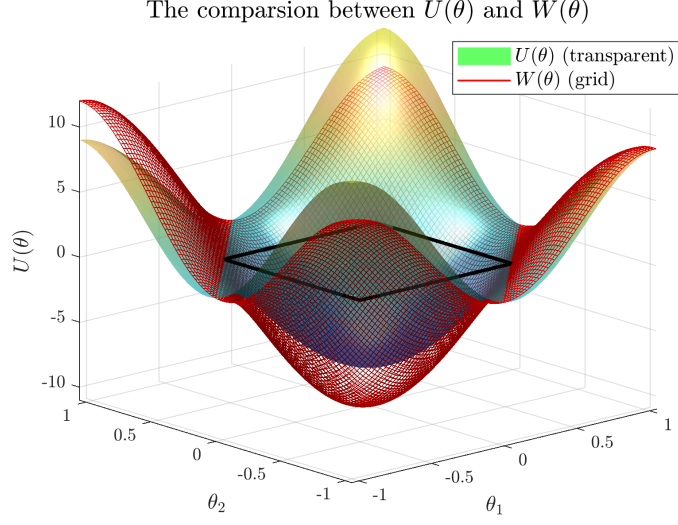


FIG. 3: The manifolds of $U(\theta)$ and $W(\theta)$ in the region of $(-\frac{\pi}{3}, +\frac{\pi}{3})_{\theta^*}^2$; $U(\theta) > W(\theta)$ in the region of $(-\frac{\pi}{6}, +\frac{\pi}{6})_{\theta^*}^2$ (black rectangle).